materials proceedings

MDPI

Proceeding Paper

Influence of Functional Groups on Their Structural Behavior Under Specific Physical and Chemical Stimuli †

Miguel A. Hernandez-Martinez [1], Lazaro Ruiz-Virgen [1], Rubén Caro-Briones [1,2], Gabriela Martínez-Mejía [1], José Manuel del Río [3,4] and Mónica Corea [1,*]

[1] Laboratorio de Investigación en Polímeros y Nanomateriales, ESIQIE, Instituto Politécnico Nacional, Av. Luis Enrique Erro S/N, Unidad Profesional Adolfo López Mateos, Zacatenco, Alcaldía Gustavo A. Madero, Ciudad de México 07738, Mexico; mahdzph22@gmail.com (M.A.H.-M.); lazaro1990@hotmail.com (L.R.-V.); rcaro@ipn.mx (R.C.-B.); gamartinezm@ipn.mx (G.M.-M.)

[2] Escuela Superior de Ingeniería Mecánica y Eléctrica, ESIME, Instituto Politécnico Nacional, Av. Luis Enrique Erro S/N, Unidad Profesional Adolfo López Mateos, Zacatenco, Alcaldía Gustavo A. Madero, Ciudad de México 07738, Mexico

[3] Escuela Superior de Física y Matemáticas, ESFM, Instituto Politécnico Nacional, Av. Luis Enrique Erro S/N, Unidad Profesional Adolfo López Mateos, Zacatenco, Alcaldía Gustavo A. Madero, Ciudad de México 07738, Mexico; jdelriog@ipn.mx

[4] Posgrado en Ingeniería en Metalurgia y Materiales, ESIQIE, Instituto Politécnico Nacional, Av. Luis Enrique Erro S/N, Unidad Profesional Adolfo López Mateos, Zacatenco, Alcaldía Gustavo A. Madero, Ciudad de México 07738, Mexico

* Correspondence: mcoreat@yahoo.com.mx or mcorea@ipn.mx; Tel.: +52-55-5729 6000 (ext. 55130 or 54239)

† Presented at the 5th International Online Conference on Nanomaterials, 22–24 September 2025; Available online: https://sciforum.net/event/IOCN2025.

Abstract

pH-thermo-responsive polymeric nanoparticles (P-Nps) functionalized with carboxylic (–COOH) and amide ($–NH_2$) groups were synthesized by emulsion polymerization to obtain two series with varying functional group ratios and morphologies: core–shell and core–concentration gradient. P-Np dispersions were characterized by dynamic light scattering (DLS), electrophoresis (zeta potential, ζ), scanning electron microscopy (SEM), and rheology (viscosity, η) in a temperature range of 25 °C to 60 °C. In general, the results show that P-Nps exhibit average particle diameters ranging from $250 \leq Dz/nm \leq 1200$, and exhibit high colloidal stability ($-46 \leq \zeta/mV \leq -22$) as temperature rises. SEM analysis revealed irregular and different structures as the proportion of functional groups varied, while rheological measurements demonstrated non-Newtonian behavior as the average shear rate increased ($0.01 \leq \dot{\gamma}/s^{-1} \leq 100$). Their size, stability, and rheological properties depend on the temperature and location of the functional groups. These properties suggest potential applications such as in stimulating fluids in the oil industry.

Keywords: emulsion polymerization; nanomaterials; smart nanoparticles; oil industry

Academic Editor: Jose L. Arias Mediano

Published: 30 December 2025

Citation: Hernandez-Martinez, M.A.; Ruiz-Virgen, L.; Caro-Briones, R.; Martínez-Mejía, G.; del Río, J.M.; Corea, M. Influence of Functional Groups on Their Structural Behavior Under Specific Physical and Chemical Stimuli. *Mater. Proc.* **2025**, *25*, 19. https://doi.org/10.3390/materproc2025025019

1. Introduction

Emulsion polymerization is a free radical technique that enables the formation of polymer particles in an aqueous dispersion with different chemical compositions; molecular weight distributions, sizes, and morphologies, such as homogeneous, Janus, and core–shell; and structures with a concentration gradient [1]. This process allows the functionalization of particles by incorporating functional groups into their chemical structure [2,3].

Chemical stimuli (pH) alter the interaction of polymers with the solvent or other polymers through the ionization of functional groups, while physical stimuli (temperature)

affect the mobility of the polymer chains [4,5]. Specifically, the incorporation of carboxylic groups (–COOH) from methyl methacrylate (MMA) or acrylic acid (AA) into the polymeric matrix provides pH sensitivity [5–7]. This behavior arises due to their ionizable nature, allowing them to accept or donate protons in response to pH variations [5,8]. As a result, the polymer undergoes a reversible compact coil-to-globule transition driven by electrostatic repulsions [5,8].

Additionally, the incorporation of amide ($–CONH_2$) or amine (NH_2) groups into the polymeric network induces conformational changes in response to external temperature variations [5–7]. The temperature at which the polymer undergoes a thermo-reversible phase transition from the swollen to the shrunken state is known as the volume phase transition temperature (VPTT) [9]. In addition, polymers exhibit a critical solution temperature (CST), which governs their miscibility in a specific solvent [5,8]. Polymer materials with a lower critical solution temperature (LCST) undergo a phase transition from a homogenous solution to a two-phase system as the temperature increases [5,8]. This transition involves a shift from a water-soluble to a water-insoluble state [5,8]. Polymeric systems with an upper critical solution temperature (UCST) suffer a phase separation upon cooling. Below the UCST, the polymer becomes less soluble, while its solubility increases as the temperature rises [5,8]. These phenomena result from the balance between hydrophobic and hydrophilic interactions within the polymer network [5,8].

Currently, multi-stimuli-responsive particles are being extensively investigated due to their ability to undergo physicochemical changes in response to multiple external stimuli [8]. Dual-stimulus-responsive polymeric particles that exhibit pH and temperature sensitivity are often synthesized by functionalizing the polymer backbone with acid (–COOH) and base ($–CONH_2$) responsive groups [10].

Recent studies have reported the use of novel, dual-stimulus-responsive polymer nanomaterials in the oil industry, particularly for acid-stimulation treatment, a well-stimulation technique used to enhance the flow of oil or gas into the wellbore without exceeding the fracture pressure of the reservoir rock [11,12]. These functionalized polymeric materials are commonly employed as stimulation fluids to mitigate corrosion, dissolve mineral deposits, and increase the permeability of oil reservoirs [13,14]. This study builds on previous studies [15,16] which evaluated the volumetric thermodynamic properties of latex systems with a total solids content of 3 wt.% and varying proportions of functional groups, as well as their responsiveness to external stimuli. The main objective was to design particles with potential applications in acid stimulation processes, focusing on their response to external stimuli and their affinity for metal ions in carbonate reservoirs [15,16].

In this work, functionalized polymeric nanoparticles (P-NPs) with a total solids content of 10 wt.% were synthesized via emulsion polymerization to obtain two series with different morphologies: core–shell and a core with a concentration gradient. The polymeric systems exhibited a significant response to external temperature changes, characterized by a reduction in particle size, colloidal stability, and viscosity as temperature increased. These behaviors are attributed to the interactions between polymer chains and solvent molecules, which are strongly influenced by the localization and concentration of functional groups within the polymer network. The results suggest that these polymer systems have potential applications in the oil industry, owing to the tunability of their properties in response to environmental variations.

2. Materials and Methods

Acrylic acid (AA) (Sigma-Aldrich, Burlington, MA, USA); acrylamide (AMm) (Sigma-Aldrich, Shanghai, China); and methyl methacrylate (MMA) (Poliformas Plásticas, Mexico City, Mexico) were used as monomers. Sodium persulfate (Sigma-Aldrich, Burlington, MA,

USA) was used as the initiator (I), and the octylphenol ethoxylate from Solvay (New York City, NY, USA) served as the surfactant (S). Distilled water (DW) (Mizu Técnica, Naucalpan de Juárez, México) was used as the solvent. Reagents were used without prior purification. The distilled water was purified using a Barnstead Micropure water purification system (Thermo Fisher Scientific Inc., Niederelbert, Germany).

2.1. Synthesis of Materials

- Smart polymer nanoparticles were synthesized via emulsion polymerization to obtain two different morphologies, as shown in Figure 1: (a) Series 1—core–shell; (b) Series 2—core–concentration gradient. The polymerization conditions are detailed in previous works [15,16]. The polymeric materials were formulated to achieve a total solids content of 10 wt.%, with 40 wt.% of functional groups. The functional groups ratios were varied as follows: 70:30 wt.%, 80:20 wt.%, and 90:10 wt.% (AA/AMm).

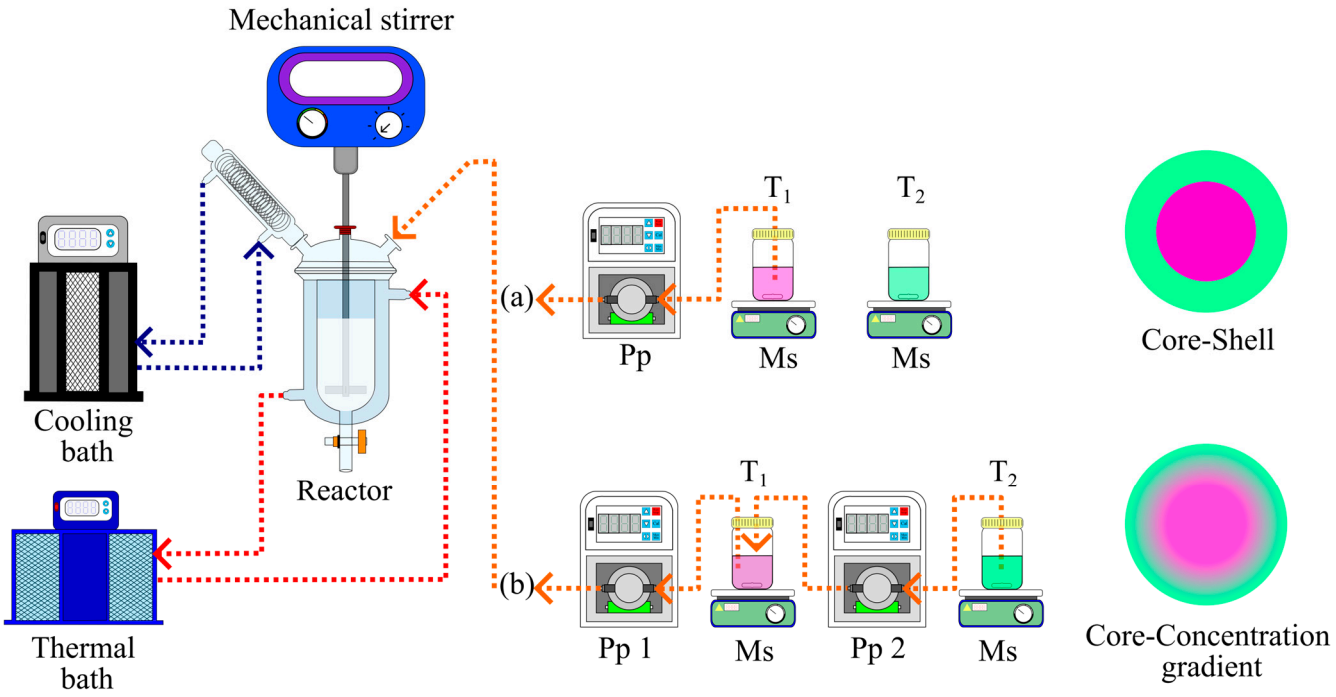

Figure 1. Polymerization process of Series 1 (**a**) and Series 2 (**b**), where Pp—peristaltic pump; T_1—Tank 1; T_2—Tank 2; Ms—mechanical stirrer; ■—carboxylic groups; ■—amide groups; ■—mixture of carboxylic amide groups.

- Nanoparticles in Series 1 (Figure 1a) were obtained by a two-stage semi-continuous process [15]. In the first stage, Tank 1 (T_1), containing a pre-emulsion solution of water, initiator, surfactant, MMA, and AA, was added to the reactor to form a core of carboxylic groups. In the second stage, the pre-emulsion from Tank 2 (T_2), which contained Amm, was added to form a shell with amide groups [15]. Nanoparticles of Series 2 (Figure 1b) were synthesized using a power feed process described by Basset et al. [15,17–19]. This sequential addition arrangement resulted in a concentration gradient of carboxylic and amide groups, using the same chemical compositions from Tank 1 and Tank 2 as in Series 1 [15,17,18].

2.2. Characterization of Nanomaterials

- The nanoparticles were characterized using several analytical techniques as part of ongoing research into their behavior, structural modifications, intra- and intermolecular

interactions with the surrounding environment under specific pH- and temperature-sensitive conditions [16].

2.2.1. Gravimetry

- The total solid content (T_s) was estimated from the slope at the trough in a plot of polymer mass (m_P) as a function of latex mass (m_L), using the gravimetry technique [18]. T_s defines the final solids content of the polymer in the dispersions. The detailed methodology is provided in a previous work [18].

2.2.2. Dynamic Light Scattering (DLS) and Electrophoresis (Zeta Potential, ζ)

- To determine particle size distribution and the ζ-potential at 25 °C, 30 °C, 40 °C, 50 °C, and 60 °C, DLS and electrophoresis techniques were employed. The experiments were conducted using a Zetasizer Nano ZSP (Malvern Instruments, Malvern, UK). The polymer nanoparticles in the dispersion were diluted to 10 ppm with deionized water, and then placed in a capillary cell (DTS1070). Measurements were performed in quadruplicate. From the particle size distribution data, the average diameter in number (D_n), weight (D_w), and hydrodynamic (D_z) were calculated using the equations described by Peter A. et al. [20]. These analyses were performed to evaluate the effect of temperature on the average particle diameter and colloidal stability.

2.2.3. Scanning Electron Microscopy (SEM)

- Scanning electron microscopy (SEM) was employed to analyze the influence of the distribution of functional groups on the morphology and surface structure of polymeric nanoparticles. The analyses were performed using a Field Emission Scanning Electron Microscope (JEOL JM-7800F, Tokyo, Japan). The latex dispersions were diluted 1:100 with deionized water (DW) and deposited onto the sample holder. Then, a gold coating was applied to the sample for 2 s. Each analysis was performed under the following conditions: secondary electron imaging at 5.0 kV, a working distance of 10 mm, and magnifications ranging from 1000 to 50,000x.

2.2.4. Rheological Properties: Viscosity (η)

- To assess the rheological properties of polymeric nanoparticles over a temperature range of 30–60 °C, the viscosity (η) of polymer dispersions without dilution was measured using a Modular Compact Rheometer MCR 502 (Anton Paar, Graz, Austria). Measurements were conducted in rotational mode with a concentric cylinder measuring system (CC27), and the shear rate ($\dot{\gamma}$) was varied from 0.01 to 1000 s^{-1}. All experiments were performed in triplicate.

3. Results and Discussion

3.1. Characterization of Nanomaterials

3.1.1. Total Solids Content (T_s) of Polymers Nanoparticles

The total solids content of the six materials was determined using the gravimetric method. The results indicate that all materials have a total solid content of approximately 9.50 ± 0.32 wt.%, confirming the accuracy of the synthesis method.

3.1.2. Average Particle Diameter (Dz) and Zeta Potential (ζ)

Figure 2 shows Dz as a function of temperature. In general, a decrease in the Dz of materials is observed. Series 1 (Figure 2a) shows that the Dz of material 70:30 wt.% is 254 nm and 354 nm at 25 °C and 40 °C, respectively. The Dz decreases up to 278 nm at 60 °C. For the material 80:20 wt.%, the largest particle (1219 nm) is observed at 30 °C. However,

the Dz is close to 618 nm at 60 °C. Finally, for the material 90:10 wt.%, no significant changes are observed in the Dz, but there is a low concentration of amide groups. This behavior is related to the amide groups located in the shell of the particles, which exhibit an LCST close to 37 °C [15,21]. This means that when the system temperature is above the LCST, a phase-volume transition is observed due to the formation of hydrophobic interactions [15,22,23]. Furthermore, hydrogen bonds and van der Waals interactions between polymer chains disrupt their interactions with water molecules, leading to a reduction in Dz [22,23].

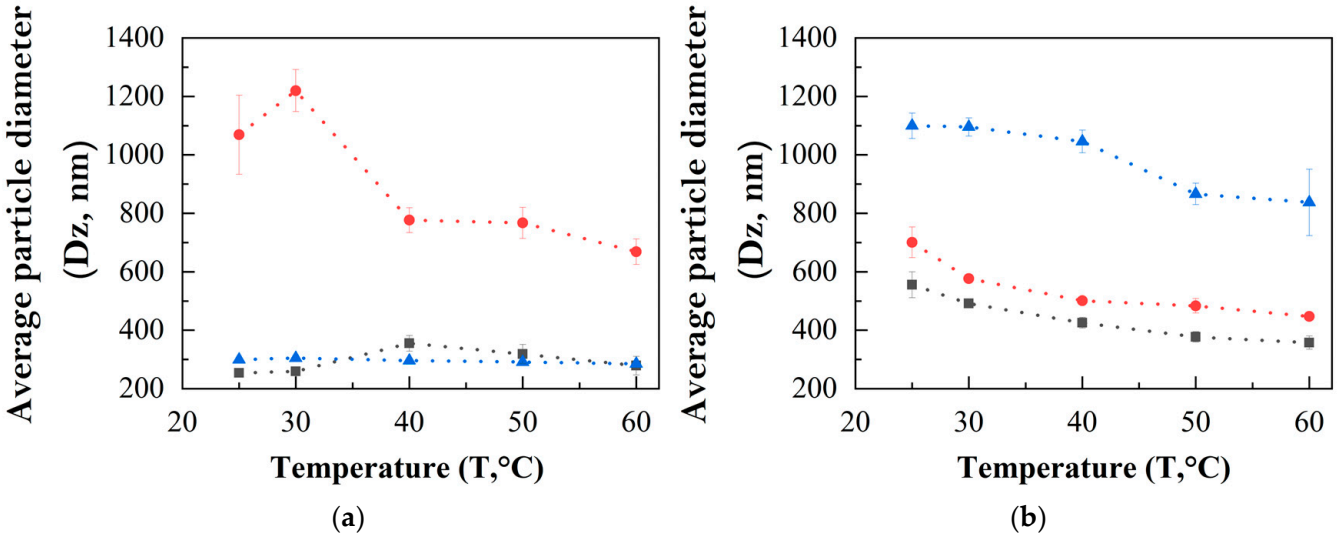

Figure 2. Average particle diameter (Dz, nm) as a function of temperature at different proportions of AA/AMm—70:30 wt.% (■), 80:20 wt.% (●), and 90:10 wt.% (▲)—for Series 1 (**a**) and Series 2 (**b**), respectively.

In Series 2 (Figure 2b), as the concentration of AA increases, the 0Dz rises due to the formation of a surface concentration gradient (AA:AMm wt.%). However, as the temperature increases, Dz decreases across all AA concentrations. This behavior is characteristic of polymer materials with a lower critical solution temperature (LCST), where Dz diminishes as hydrophobicity increases. This enhanced hydrophobicity strengthens the interactions between functional groups and polymer chains through van der Waals forces, leading to particle aggregation [24].

Figure 3 shows the ζ values as a function of temperature for both series. Negative values of ζ are attributed to the negative charges caused by the dissociation and ionization of carboxylic groups (–COOH) into anions ($–COO^-$), and neutral charges of amide groups ($–CONH_2$) present in the polymer chains of particles [25]. According to the literature, colloidal systems are stable when the zeta potential values are > ±30 mV [15,25,26]. For Series 1 (Figure 3a), the zeta potential values range from −46 to −26 mV, while for Series 2 (Figure 3b), ζ values range from −40 to −22 mV. Particle stability decreases above 40 °C, when the temperature of the system exceeds the LCST of ~37 °C. This phenomenon is attributed to the disruption of hydrogen bonds and van der Waals forces between polymer chains, which reduces the availability of functional groups for interaction with the environment, leading to particle contraction and a loss of colloidal stability [15,24].

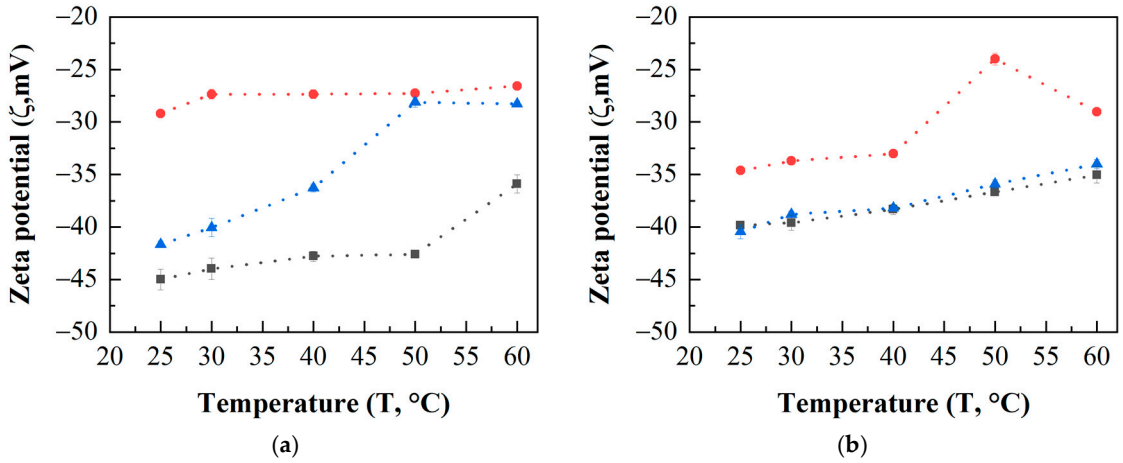

Figure 3. Zeta potential (ζ, mV) as a function of temperature at different proportions of AA/AMm—70:30 wt.% (■), 80:20 wt.% (●), and 90:10 wt.% (▲)—for Series 1 (**a**) and Series 2 (**b**), respectively.

3.1.3. Scanning Electron Microscopy of Polymers Nanoparticles

The superficial morphology of the nanoparticles was observed using scanning electron microscopy (SEM). In Series 1, the 70:30 wt.% material (Figure 4a) exhibits an irregular and anisotropic structure with a striated surface. The 80:20 wt.% material (Figure 4b) shows a pseudo-spherical structure, while the 90:10 wt.% material (Figure 4c) presents larger structures with a "popcorn" morphology and a rough surface [27]. In Series 2, the 70:30 wt.% (Figure 4d) and 80:20 wt.% (Figure 4e) materials exhibit a "popcorn" morphology with a hole-like structure whereas the 90:10 wt.% material (Figure 4f) displays a cauliflower morphology [28]. Both series show an increase in particle size at higher AA concentrations, which is attributed to the formation of larger particles at elevated AA concentrations [28]. Additionally, the particle morphology is influenced by the synthesis method and the localization of functional groups [27].

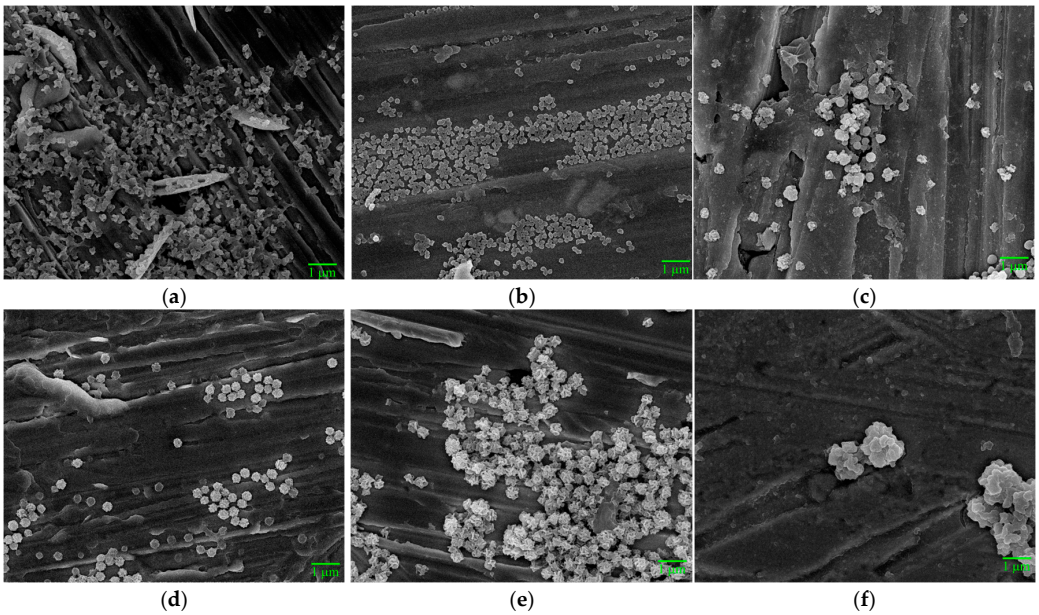

Figure 4. Micrographs of nanoparticles at 10,000x magnification at different proportions of AA/AMm—70:30 wt.% (**a**,**d**), 80:20 wt.% (**b**,**e**), and 90:10 wt.% (**c**,**f**)—for Series 1 and Series 2, respectively.

3.1.4. Rheology Properties of Polymers Nanoparticles

Oscillatory rheology was used to evaluate the viscous properties of latex [29].

Viscosity of Polymers Nanoparticles

All dispersions exhibited a decrease in viscosity as temperature increased, a trend observed across all polymers, particularly those with lower acrylic acid (AA) concentrations. Figure 5a,b shows the viscosity as a function of shear rate at 30 °C, 40 °C, 50 °C, and 60 °C for the 70:30 wt.% materials from Series 1 and Series 2, respectively. As the temperature approaches the LCST of ~37 °C, the particles contract, resulting in a reduction in particle size, flow resistance, and viscosity [21,30,31]. Polymeric dispersions display two distinct behaviors during the stress sweep; (i) at $0.01 \leq \dot{\gamma}/s^{-1} \leq 10$, the dispersions undergo thinning due to particle alignment in the flow and the breakup of polymer chain interactions (van der Waals and hydrogen bonds) [31], and (ii) between 10 and 100 s^{-1}, they exhibit a Newtonian behavior, with viscosity linearly dependent on shear-induced chain alignment [29,30,32].

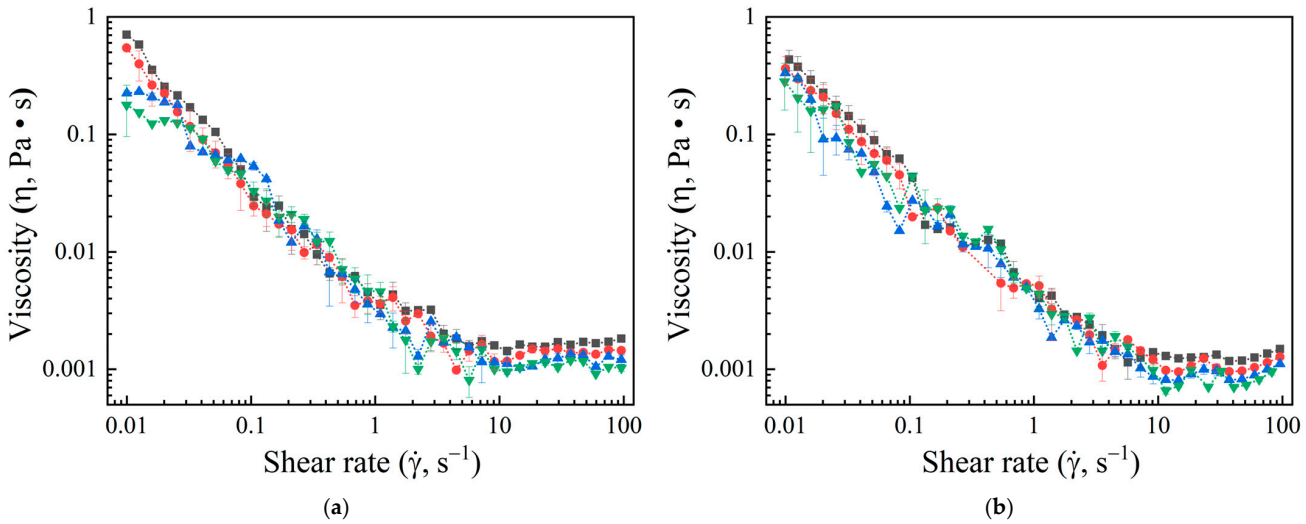

Figure 5. Viscosity (η) as a function of shear rate ($\dot{\gamma}$) of latex 70:30 wt.%–AA/AMm wt.% at different temperatures—30 °C (■), 40 °C (●), 50 °C (▲), and 60 °C (▼)—for Series 1 (**a**) and Series 2 (**b**).

4. Conclusions

Polymeric materials exhibit typical characteristics of smart materials, such as pH and thermo-responsiveness, along with high stability. As temperature increases, a decrease in particle size (Dz) and viscosity is observed, particularly for materials near their LCST, which is attributed to enhanced hydrophobic interactions and particle contraction. Zeta potential analysis shows stable colloidal systems, although particle stability decreases above the LCST due to disruptions in polymer chain interactions. SEM analysis reveals distinct morphologies, including "popcorn" and "cauliflower" structures, influenced by the concentration of AA and the functional group distribution. Overall, these characteristics make the materials suitable for use in the oil industry (acidification processes), where controlled particle behavior and colloidal stability are crucial.

Author Contributions: Conceptualization, J.M.d.R. and M.C.; methodology, M.A.H.-M.; validation, L.R.-V., R.C.-B., J.M.d.R. and M.C.; formal analysis, M.A.H.-M., L.R.-V., R.C.-B., G.M.-M. and M.C.; investigation, M.A.H.-M.; resources, L.R.-V. and M.C.; data curation, M.A.H.-M.; writing—original draft preparation, M.A.H.-M.; writing—review and editing, M.A.H.-M. and L.R.-V.; visualization, M.A.H.-M.; supervision, L.R.-V. and M.C.; project administration, J.M.d.R. and M.C. All authors have read and agreed to the published version of the manuscript.

Funding: This research received no external funding.

Institutional Review Board Statement: Not applicable.

Informed Consent Statement: Not applicable.

Data Availability Statement: The original contributions presented in this study are included in the article. Further inquiries can be directed to the corresponding author.

Acknowledgments: The authors would like to acknowledge CENTRO DE NANOCIENCIAS Y MICRONANOTECNOLOGÍAS (CNMN, IPN) and the ESCUELA SUPERIOR DE INGENIERÍA QUÍMICA E INDUSTRIAS ECTRACTIVAS (ESIQIE, IPN) for their characterization techniques.

Conflicts of Interest: The authors declare no conflicts of interest.

References

1. Priestley, R.; Prud'homme, R. (Eds.) *Polymer Colloids: Formation, Characterization and Applications*; Soft Matter Series; Royal Society of Chemistry: Cambridge, UK, 2019. [CrossRef]
2. Elaissari, A. (Ed.) *Colloidal Polymers: Synthesis and Characterization*; Surfactant Science Series, no. v. 115; M. Dekker: New York, NY, USA, 2003.
3. Mosnáčková, K.; Kollár, J.; Huang, Y.-S.; Huang, C.-F.; Mosnáček, J. Synthesis Routes of Functionalized Nanoparticles. In *Polymer Composites with Functionalized Nanoparticles*; Elsevier: Amsterdam, The Netherlands, 2019; pp. 1–46. [CrossRef]
4. Fattah-Alhosseini, A.; Chaharmahali, R.; Alizad, S.; Kaseem, M.; Dikici, B. A review of smart polymeric materials: Recent developments and prospects for medicine applications. *Hybrid Adv.* **2024**, *5*, 100178. [CrossRef]
5. Aguilar, M.R.; Román, J.S. (Eds.) Smart polymers and their applications, Second edition. In *Woodhead Publishing in Materials*; Woodhead Publishing: Duxford, UK; Cambridge, MA, USA, 2019.
6. He, Y.; Gou, S.; Zhou, Y.; Zhou, L.; Tang, L.; Liu, L.; Fang, S. Thermoresponsive behaviors of novel polyoxyethylene-functionalized acrylamide copolymers: Water solubility, rheological properties and surface activity. *J. Mol. Liq.* **2020**, *319*, 114337. [CrossRef]
7. Jalababu, R.; Veni, S.S.; Reddy, K.S. Synthesis and characterization of dual responsive sodium alginate-g-acryloyl phenylalanine-poly N -isopropyl acrylamide smart hydrogels for the controlled release of anticancer drug. *J. Drug Deliv. Sci. Technol.* **2018**, *44*, 190–204. [CrossRef]
8. Abouelmagd, S.A.; Ellah, N.H.A.; El Hamid, B.N.A. Temperature and pH dual-stimuli responsive polymeric carriers for drug delivery. In *Stimuli Responsive Polymeric Nanocarriers for Drug Delivery Applications*; Elsevier: Amsterdam, The Netherlands, 2019; pp. 87–109. [CrossRef]
9. Suljovrujic, E.; Miladinovic, Z.R.; Krstic, M. Swelling properties and drug release of new biocompatible POEGOPGMA hydrogels with VPTT near to the human body temperature. *Polym. Bull.* **2020**, *78*, 2405–2425. [CrossRef]
10. Kalhapure, R.S.; Renukuntla, J. Thermo- and pH dual responsive polymeric micelles and nanoparticles. *Chem. Interact.* **2018**, *295*, 20–37. [CrossRef]
11. de Leon, A.C.C.; da Silva, Í.G.; Pangilinan, K.D.; Chen, Q.; Caldona, E.B.; Advincula, R.C. High performance polymers for oil and gas applications. *React. Funct. Polym.* **2021**, *162*, 104878. [CrossRef]
12. Mittal, V. *Polymers in Oil and Gas Industry*; Central West Publishing: Orange, NSW, Australia, 2018; ISBN 978-0-6482205-0-3.
13. Adewunmi, A.A.; Solling, T.; Sultan, A.S.; Saikia, T. Emulsified acid systems for oil well stimulation: A review. *J. Pet. Sci. Eng.* **2022**, *208*, 109569. [CrossRef]
14. Tiu, B.D.B.; Advincula, R.C. Polymeric corrosion inhibitors for the oil and gas industry: Design principles and mechanism. *React. Funct. Polym.* **2015**, *95*, 25–45. [CrossRef]
15. Ruiz-Virgen, L.; Hernández-Martínez, M.A.; Martínez-Mejía, G.; Caro-Briones, R.; del Río, J.M.; Corea, M. Study of Thermodynamic and Rheological Properties of Sensitive Polymeric Nanoparticles as a Possible Application in the Oil Industry. *J. Solut. Chem.* **2024**, *53*, 5–27. [CrossRef]
16. Ruiz-Virgen, L.; Hernandez-Martinez, M.A.; Martínez-Mejía, G.; Caro-Briones, R.; Herbert-Pucheta, E.; del Río, J.M.; Corea, M. Analysis of Structural Changes of pH–Thermo-Responsive Nanoparticles in Polymeric Hydrogels. *Gels* **2024**, *10*, 541. [CrossRef] [PubMed]
17. Santillán, R.; Nieves, E.; Alejandre, P.; Pérez, E.; del Río, J.; Corea, M. Comparative thermodynamic study of functional polymeric latex particles with different morphologies. *Colloids Surf. A Physicochem. Eng. Asp.* **2014**, *444*, 189–208. [CrossRef]
18. Santillán, R.; Nieves, E.; Alejandre, C.; Gómez-Yañez, C.; del Río, J.; Dorantes-Rosales, H.; Navarro-Clemente, M.; Corea, M. Synthesis of highly carboxylated latex particles using a power feed process. *J. Ind. Eng. Chem.* **2012**, *19*, 1257–1266. [CrossRef]
19. *Emulsion Polymers and Emulsion Polymerization*; American Chemical Society (ACS): Washington, DC, USA, 1981; ISBN 9780841206427.

20. Lovell, P.A.; Schork, F.J. Fundamentals of Emulsion Polymerization. *Biomacromolecules* **2020**, *21*, 4396–4441. [CrossRef] [PubMed]
21. Zeinali, E.; Haddadi-Asl, V.; Roghani-Mamaqani, H. Nanocrystalline cellulose grafted random copolymers of N-isopropylacrylamide and acrylic acid synthesized by RAFT polymerization: Effect of different acrylic acid contents on LCST behavior. *RSC Adv.* **2014**, *4*, 31428–31442. [CrossRef]
22. Zhao, C.; Dolmans, L.; Zhu, X.X. Thermoresponsive Behavior of Poly(acrylic acid-*co*-acrylonitrile) with a UCST. *Macromolecules* **2019**, *52*, 4441–4446. [CrossRef]
23. Le, M.; Huang, W.; Chen, K.-F.; Lin, C.; Cai, L.; Zhang, H.; Jia, Y.-G. Upper critical solution temperature polymeric drug carriers. *Chem. Eng. J.* **2022**, *432*, 134354. [CrossRef]
24. Najafi, M.; Habibi, M.; Fokkink, R.; Hennink, W.E.; Vermonden, T. LCST polymers with UCST behavior. *Soft Matter* **2021**, *17*, 2132–2141. [CrossRef]
25. Mekewi, M.A.; Madkour, T.M.; Darwish, A.S.; Hashish, Y.M. Does poly(acrylic acid-co-acrylamide) hydrogel be the pluperfect choiceness in treatment of dyeing wastewater? "From simple copolymer to gigantic aqua-waste remover". *J. Ind. Eng. Chem.* **2015**, *30*, 359–371. [CrossRef]
26. Bhattacharjee, S. DLS and zeta potential—What they are and what they are not? *J. Control. Release* **2016**, *235*, 337–351. [CrossRef]
27. Abdollahi, A.; Roghani-Mamaqani, H.; Salami-Kalajahi, M. Morphology evolution of functionalized styrene and methyl methacrylate copolymer latex nanoparticles by one-step emulsifier-free emulsion polymerization. *Eur. Polym. J.* **2020**, *133*, 109790. [CrossRef]
28. Jamali, A.; Moghbeli, M.R.; Ameli, F.; Roayaie, E.; Karambeigi, M.S. Synthesis and characterization of pH-sensitive poly(acrylamide-*co*-methylenebisacrylamide-*co*-acrylic acid) hydrogel microspheres containing silica nanoparticles: Application in enhanced oil recovery processes. *J. Appl. Polym. Sci.* **2019**, *137*, e48491. [CrossRef]
29. Nesrinne, S.; Djamel, A. Synthesis, characterization and rheological behavior of pH sensitive poly(acrylamide-co-acrylic acid) hydrogels. *Arab. J. Chem.* **2017**, *10*, 539–547. [CrossRef]
30. Reis, B.M.; Armes, S.P.; Fujii, S.; Biggs, S. Characterisation of the dispersion stability of a stimulus responsive core–shell colloidal latex. *Colloids Surf. A Physicochem. Eng. Asp.* **2010**, *353*, 210–215. [CrossRef]
31. Buratti, E.; Franco, S.; Di Gregorio, G.; Ripanti, F.; Nigro, V.; Bertoldo, M.; Angelini, R.; Postorino, P.; Ruzicka, B. Copolymer vs interpenetrated polymer network microgels: The case of poly(N-isopropylacrylamide) and poly(acrylic acid). *J. Mol. Liq.* **2025**, *427*, 127328. [CrossRef]
32. de Vasconcelos, C.K.; Lopes, R.C.; Medeiros, F.S.; Viana, M.M.; Caliman, V.; Silva, G.G. Rheological and structural properties of nanofluids based on hydrolyzed polyacrylamide and aminated carbon nanotubes for enhanced oil recovery. *Polymer* **2024**, *307*, 127325. [CrossRef]